A Competitive Kinetic Model of Nucleic Acid Surface Hybridization in the Presence of Point Mutants

J. Bishop, S. Blair, and A. M. Chagovetz

Department of Electrical and Computer Engineering University of Utah, Salt Lake City, Utah

ABSTRACT   Microarray analysis has become increasingly complex due to the growing size of arrays and the inherent cross-binding of targets. In this work, we explore the effects of matched and mismatched target species concentrations, temperature, and the time of hybridization on sensing specificity in two-component systems. A finite element software is used to simulate the diffusion of DNA through a microfluidic chamber to the sensing surface where hybridization of DNA is modeled using the corresponding kinetic equation. Comparison between a single-component system, where only one target is allowed to bind to a specific zone, and a two-component system, where more than one target can hybridize in a sensing zone, uncovers significant kinetic disparities during the transitory state; however, at thermodynamic equilibrium a modified Langmuir isotherm governs the bound amount of both species. The results presented suggest that it may be more appropriate to consider collective rather than quasi-independent interaction of targets in multicomponent systems.

INTRODUCTION

Systemic approaches in genetic research, molecular diagnostics, and pharmacogenetics motivate the need for multitarget nucleic acid arrays with high sensitivity and selectivity. Arrays are also needed in the clinical application of genetic screening for the rapid identification of genetic disorders in the presence of multiple genotypes and/or mutations (1,2). Numerous statistical models have been created to evaluate the hybridization of nucleic acid targets using end-point analysis (3,4). Additionally, several authors have proposed mechanistic models of single-component hybridization combining mass transport of target and chemical interactions on the surface of the array (5–9).

Several groups have been active in analyzing the kinetic behavior of surface capture (10–13). Their efforts resulted in an emerging consensus theoretical approach, which addresses the effects of three-dimensional and two-dimensional (surface-bound) mass transport, and surface chemistry, i.e., probe interactions, probe density, and steric hindrances by introducing efficient (or apparent) rate constants or more complicated rate functional parameters. The important result of these studies is in defining surface and solution boundary conditions at which some of these effects may be neglected in a kinetic model. It was found that at probe densities of $<10^{12}/cm^2$, probe-probe interactions and molecular crowding effects are insignificant. However, all of these studies use a single analyte case for building the models, which limits their applicability in interpreting multicomponent microarray data. Although Erickson et al. (12) looked at differences in kinetic capture of point mutants and wild-type targets, these cases were treated as separate capture experiments.

In this work, we explore the effects of target and mismatched species concentrations, temperature, and the time of hybridization on sensing specificity in two-component systems. A finite element method is used to simulate the diffusion of DNA through a microfluidic chamber to the sensing surface where hybridization of DNA is modeled using the corresponding chemical reaction equation assuming low grafting density. The association rate constant for the 20-mer sequences is obtained from experimental data for the perfect match target, and is used along with a thermodynamic model to determine dissociation rate constants at different temperatures. One system evaluated is a two-component solution consisting of a wild-type 20-mer sequence and a single nucleotide polymorphism (SNP) mismatch. Another scenario evaluates the binding of the wild-type strand and a strand which had a two- or three-basepair mismatch. Simulation results and the solution to the two-component chemical reaction equations were utilized to evaluate the time needed to reach equilibrium. Additionally, the dynamics of a two-component system versus those of a single-component system are dissected and the impact on analysis is discussed. Time to reach equilibrium is proposed as a useful metric to quantitate kinetic competition effects. We show that time to equilibrium is significantly elongated in competitive hybridizations compared to single-component capture. This finding challenges the validity of equilibrium assumptions by current analysis approaches.

THEORY

Mathematical model: single species

Nucleic acid arrays employ affinity interactions between complementary strands as the mechanism for sensing. Target which is delivered to the sensing surface from solution via diffusion is interrogated by probes tethered to the sensing surface. The delivery of analyte to the surface is governed by Fick's Law (neglecting the convection term),

---

$$\frac{\partial C}{\partial t} = D\nabla^2 C, \tag{1}$$

where C is the concentration of target in solution and D is the diffusion coefficient for the target. The affinity interaction at the sensing zone, in the case of a single species, can be expressed by

$$\frac{dB}{dt} = k_a C(R_t - B) - k_d B, \tag{2}$$

where k_a represents the association rate constant, k_d is the dissociation rate constant, R_t is the initial surface concentration of probes, and B is the surface concentration of bound targets. The hybridization process in which target can bind to or melt off the surface is controlled by both diffusion and the chemical reaction at the surface. Both mass transport (diffusion) and reaction kinetic equations are included in our model. At high concentrations (nM), the mass transport contribution is insignificant compared to hybridization kinetics, whereas at low concentration (pM), it becomes the dominant contributor. Our diffusion-reaction model allows running virtual experiments without making any prior assumptions with respect to the relative contribution of each mechanism.

Eq. 2 can be solved for thermodynamic equilibrium by setting $(dB)/dt = 0$, with the resulting Eq. 3:

$$B = \frac{k_a C R_t}{k_a C + k_d}. \tag{3}$$

Under the assumption of irreversible binding, $k_a C >> k_d$ and $C > R_t$, the equilibrium-bound concentration will be equal to R_t. When k_d is comparable to $k_a C$, the bound concentration will be $< R_t$.

For the simulation results described below, the association constant for the wild-type sequence, CGCGGGCCGCATTAATAAAC, was taken to be $10^6 \text{ M}^{-1} \text{ s}^{-1}$, which was experimentally determined (14). Additional support for the value of association rate constant used in our model comes from studies of Erickson et al. (12), who demonstrated an association rate constant on the same order of magnitude due to enhanced surface diffusion extracted from experimental results (12). Similar values were used by Hagan and Chakraborty (13) for theoretical studies of nucleation rates at the surface of the sensor and also by Myszka et al. (14) on surface plasmon sensors (13,15). It is assumed that the association constant does not change greatly, more than an order of magnitude, over the temperature range used in our simulations (16). To calculate an appropriate k_d value for a specified temperature we use a thermodynamic model as illustrated in Fig. 1. This model is correct for solution-based hybridization. Although thermodynamic parameters for the surface-based reactions may be different (17–19), we use the solution approximation to study functional dependencies, which should be similar for solution and surface reactions.

Entropy (ΔS) and enthalpy (ΔH) values are calculated using MeltCalc and we assumed that they did not change with temperature (T). These values are then used to calculate ΔG, the standard free energy difference for hybridized/melted duplexes,

$$\Delta G(T) = \Delta H - (\Delta S * T). \tag{4}$$

Using

$$\Delta G^\dagger = -\log(k_a) R T_o, \tag{5}$$

the activation energy needed for hybridization was calculated using the association constant and temperature, T_o, at 298 K. The standard free energy and hybridization activation energy were used to calculate the dissociation rate constant for specific temperatures,

$$k_d(T) = \exp\left[-\frac{\Delta G^\dagger + \Delta G(T)}{RT}\right]. \tag{6}$$

Different DNA sequences could have been chosen for this study, which would have affected the values of the rate constants (20,21), and therefore
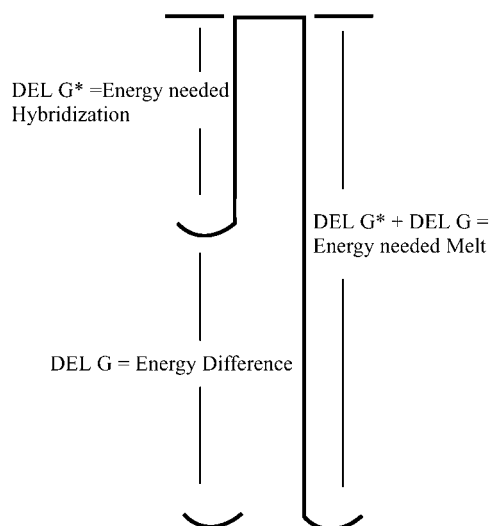
FIGURE 1 Representation of activation energies for the thermodynamic model used to calculate the dissociation constants.

would have changed the absolute values of parameters investigated: temperature dependencies, relative concentration effects, and times to reach equilibrium. Such effects would be caused by increasing the length of the strand or changing the sequence complexity. These changes could also induce secondary structures, where there are multiple competitions among the formation of different hybrids (intra- versus intermolecular) which are not accounted for in our model. For these cases, calculations of thermodynamic functions and, consequently, relative concentrations of different species should be accomplished by using a statistical thermodynamic approach, which was recently revised and updated by Dimitrov and Zuker (22). Partition functions calculations may be accomplished by using DINAMelt Server (23). However, as long as the ratios of apparent rate constants and concentration are similar to those presented here, the trends shown hold and the overall process of detection may be described in terms of the time to the thermodynamic equilibrium. This model can equally be applied to other multicomponent systems with different capture affinities: small deletion, insertions, and truncations, for example.

Mathematical model: two species

The description of a system with two species (e.g., a perfect match and a mismatch) that are mixed together, and allowed to bind to the surface, can be described by a system of equations similar to those used for only a single species. The model for the diffusion of both species is described by a system of independent diffusion equations,

$$\frac{\partial C^m}{\partial t} = D\nabla^2 C^m, \tag{7}$$

$$\frac{\partial C^{mis}}{\partial t} = D\nabla^2 C^{mis}, \tag{8}$$

where C^m corresponds to the concentration of the perfectly matched target and C^{mis} corresponds to the concentration of the mismatch. Equation 2, however, does get modified to handle a system of two species. The equations have to reflect the loss of available binding sites due to both the match and mismatch,

$$\frac{dB^m}{dt} = k_a^m C^m (R_t - B^m - B^{mis}) - k_d^m B^m, \tag{9}$$

$$\frac{dB^{mis}}{dt} = k_a^{mis} C^{mis} (R_t - B^m - B^{mis}) - k_d^{mis} B^{mis}, \tag{10}$$

where B^{m} is the bound concentration by the match, and B^{mis} is the bound concentration by the mismatch, with the corresponding association and dissociation terms. The $(R_{\mathrm{t}} - B^{\mathrm{m}} - B^{\mathrm{mis}})$ term represents the loss of probe sites due to binding of both the match and mismatch targets, and therefore couples the two equations.

The thermodynamic equilibrium solution to Eqs. 9 and 10 is more complicated than its single-species partner. The modified Langmuir isotherm for the match target, Eq. 11, shows the complexity of a multitarget solution. Equation 11, assuming that $k_{\mathrm{a}}^{\mathrm{m}} C^{\mathrm{m}}$ is much larger than $k_{\mathrm{a}}^{\mathrm{mis}} C^{\mathrm{mis}}$, simplifies to Eq. 3. However, if $k_{\mathrm{a}}^{\mathrm{m}} C^{\mathrm{m}}$ is comparable to $k_{\mathrm{a}}^{\mathrm{mis}} C^{\mathrm{mis}}$, we see that the amount bound by the match is influenced largely by the bound mismatch. The corresponding equation for bound mismatch is the same as Eq. 11, except all the indexes *mis* and *m* terms are interchanged:

$$B^{\mathrm{m}} = \frac{R_{\mathrm{t}} k_{\mathrm{a}}^{\mathrm{m}} C^{\mathrm{m}} k_{\mathrm{d}}^{\mathrm{mis}}}{k_{\mathrm{a}}^{\mathrm{m}} C^{\mathrm{m}} k_{\mathrm{d}}^{\mathrm{mis}} + k_{\mathrm{a}}^{\mathrm{mis}} C^{\mathrm{mis}} k_{\mathrm{d}}^{\mathrm{m}} + k_{\mathrm{d}}^{\mathrm{m}} k_{\mathrm{d}}^{\mathrm{mis}}}. \tag{11}$$

Note that the equilibrium bound concentration of the matched target is a function of association rate and dissociation rate ratios for matched and mismatched targets.

Numerical model

Numerical simulations of an isolated spot on a microarray were performed with FEMLab, a finite element package. The diffusion model within FEMLab was applied to a two-dimensional channel. The channel was 1-mm-long and had a height of 100 μm, as shown in Fig. 2. The sensing zone was described by a 200-μm surface centered on the bottom of the channel. The channel mesh was no larger than 10 μm and around the sensing zone the mesh was smaller than 0.1 μm. The location of the zone in the two-dimensional channel was coupled to a one-dimensional structure using a flux boundary condition. The one-dimensional structure used the diffusion model to simulate the affinity reaction between the target and probe.

No target should be lost from the top of the channel, so that boundary was set to an insulation (nonreactive) boundary. The bottom of the channel, except where the sensing zone was located, was also set to an insulation boundary. The two vertical walls on each end of the channel were set to a continuous concentration boundary. This was done to simulate the unlimited supply of target in a bulk sensor. In the case of a single target in solution, one diffusion equation is used, but with two species, two diffusion equations had to be solved. The corresponding boundary condition set the vertical walls to the appropriate concentrations and the sensing zone to the corresponding
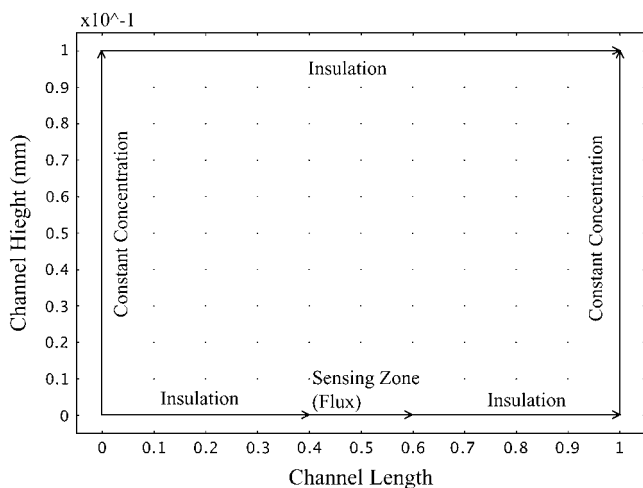
binding equation. The rate constants for association (10^6 M^{-1} s^{-1}) and dissociation (see Fig. 3) as well as the initial probe concentration (10^{-11} Mm) were entered as constants and used to solve for a time-dependent solution. The low probe density was chosen to simulate conditions under which the possible effects of electrostatic probe-probe interactions (24) and steric hindrances during target-probe hybridization could be assumed negligible (12,25). Non-Langmuir binding, which may be a result of heterogeneity in binding energies in the sensing zone, has been observed for higher submicromolar and micromolar target concentrations (26). These effects are not accounted for in our model due to the low target concentrations investigated. The initial conditions used by the time-dependent solver were $B^{\mathrm{m}} = B^{\mathrm{mis}} = 0$, and C^{m} and C^{mis} are equal to the concentration of match/mismatch target in solution.

SIMULATION RESULTS

Temperature effects

We conducted simulations to investigate the effects of temperature on hybridization kinetics for both single and two-component systems. Under the assumptions of the theoretical model, the association rate constants for matched and mismatched targets are similar and their temperature dependence in the interval under investigation (300–340 K) is within one order of magnitude; therefore k_{a} was set to a constant over all ranges of temperatures and target species. However, the dissociation constants are affected by temperature significantly. The corresponding dissociation constants for different temperatures are shown in Fig. 3 for the match and multiple mismatch sequences ranging from 1 SNP to 3 SNPs: CGCGGGC**T**GCATTAATAAAC, CGCG**A**GCCGCATT**G**ATAAAC, and CGCG**A**GCCGCA**CTG**ATAAAC. Note that the dissociation constants for the mismatch targets are always higher than those for the match target, which reflects the greater instability of the heteroduplexes as compared to the homoduplex at the same temperature.

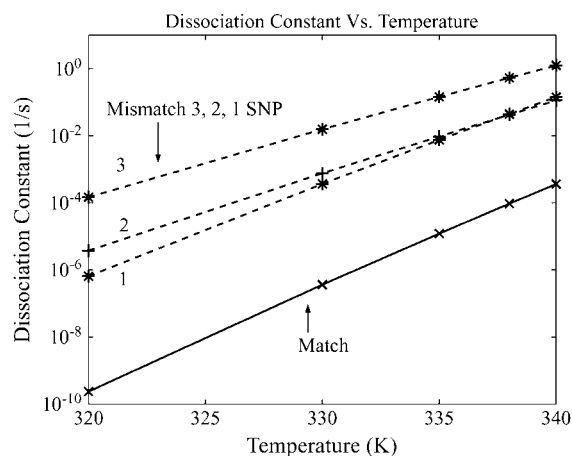Virtual experiments were performed using the two-component model for temperatures shown in Fig. 3 to

FIGURE 2 Two-dimensional channel design with the boundary conditions for each wall.

FIGURE 3 Dissociation rate constants at different temperatures for the match (*solid line*), and a 3-, 2-, or 1-SNP mismatch target (*dashed line*).

represent binding in a 20-min period. Twenty-minute binding simulations were chosen due to limitations of the finite element package in handling dissociation at high temperatures. The match/mismatch bound concentration ratios are shown in Fig. 4. Simulations were performed using equal concentrations, 100 pM, of input species. As the temperature increases, 20 K from 320 K, the amount of the 1-SNP mismatch target bound to the surface, within the simulated 20-min time span, decreases whereas the matched target bound concentration increases, leading to the increase shown in Fig. 4. This result demonstrates the effects the dissociation rate constant has on binding kinetics and suggests that a competitive binding mechanism is controlling the binding rate of the perfectly matched target.

Single versus competitive hybridization

Hybridization curves for a match target simulated in a single-component solution and match target simulated in a two-component solution, containing equimolar amounts of 1 SNP, are shown in Fig. 5 A. In addition, Fig. 5 B shows binding of a 1-SNP mismatch target in a single-component system and a 1-SNP mismatch target in a two-component system. The initial target concentration of both the match/mismatch are set to 100 pM, the modeled temperature is 330 K, and simulations depict binding for 80 h. At this temperature and hybridization time our results show that there is insignificant difference between the binding of the matched targets either in the absence or presence of mismatched species. However, there are considerable differences in the mismatch curves. The single-component simulations show that the bound mismatch displays monotonous growth over time. When both the matched and mismatched species are present we observe biphasic behavior from the bound mismatch target, where initial growth is followed by the drop-off of the bound mismatched species.
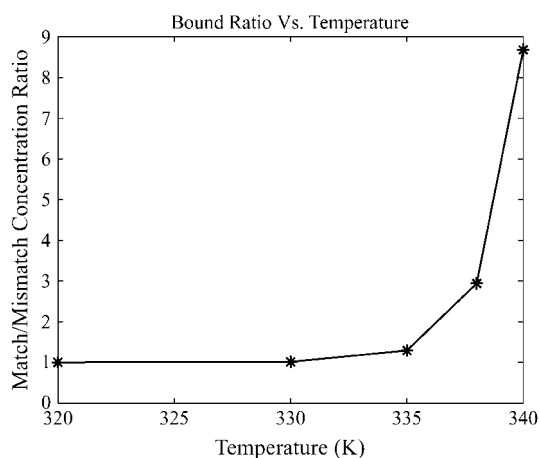
In an actual experimental setup, where a two-component system is being used, the hybridization curves shown in Fig. 5 would not be observed. Instead, a composite hybridization curve resulting from the superposition of the homoduplex and heteroduplex would be seen. Fig. 6 A shows the example of an apparent binding curve using the same input variables as stated for Fig. 5. If we analyze the composite signal using the assumption that mismatch binding is negligible, then the corresponding results would be incorrect unless thermodynamic equilibrium is reached before signal acquisition. Fig. 6 B shows the composite and match hybridization curves for an experiment where the 1-SNP mismatch concentration is 10-times higher at 1 nm than the match concentration (100 pM).

Nonspecific spots have been proposed as a means to help quantify the amount of matched target that has bound to the sensing surface. This is accomplished by subtracting the signal from a nonspecific spot from the signal of the perfectly matched spot. To simulate this technique, we allowed the 1 SNP from the match spot to have the same parameters for a nonspecific spot. The results are shown in Fig. 7 A. Over the first 20 h, there is no significant difference between the actual match curve and the curve created by subtracting the single mismatch from the composite curve (i.e., the false match), but at longer time the difference becomes more prominent. This scenario would be the best case where the matched target has no affinity to the nonspecific spot. If the match does have a non-zero affinity to the nonspecific zone, then the amount of bound target to the nonspecific spot would have to be modeled by the two-component model. This has been completed simulating effects using the 1 SNP from the match spot as the 1 SNP for the nonspecific spot and the match target as a 2 SNP for the nonspecific spot with results shown in Fig. 7 B. This result shows that there is a major difference between the actual match and the one that would be calculated even at short times. This result would be even more exaggerated if the 1-SNP mismatch were at a concentration 10-times higher than the perfectly matched target. Such a case would suggest that there was basically no matched target in solution for times shorter than 10 h.

Time to thermodynamic equilibrium

Thermodynamic equilibrium can be defined as the point at which the amount of a species bound to the surface does not change with time or when there is equal probability that a target will bind to or melt off the surface. Using Eq. 11, the thermodynamic equilibrium bound surface concentration was calculated for the matched target. This was then used to find out how long it would take to reach equilibrium at the temperature of 330 K, using varying relative combination of concentrations of matched and mismatched species. Table 1 shows the results of the investigation. Note that the single-component case is included as a reference. As the concentration of both the match and 1-SNP mismatch increase, the
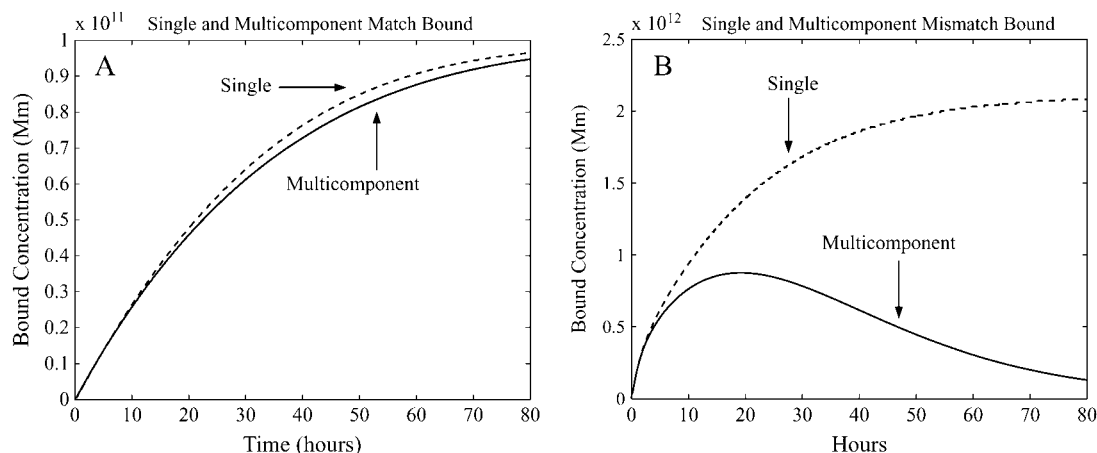

FIGURE 4 Ratio of bound concentration of match and 1-SNP mismatch after 20 min of hybridization at different temperatures.

FIGURE 5 Hybridization curves simulating target concentrations at 100 pM at a temperature of 330 K. (*A*) Match targets simulated in single (*dashed line*) and two-component (*solid line*) systems; and (*B*) mismatch targets simulated in single (*dashed line*) and two-component (*solid line*) systems.

time to completion decreases; however, if the concentration of the mismatch increases while the concentration of the match stays constant, the time to completion increases. The long times needed to reach 90% of thermodynamic equilibrium are not acceptable, unless experiments are done at concentrations that are higher than 1 nM concentration for both match and mismatch targets.

Simulations of equal concentrations of targets are valuable in understanding the mechanism of a hybridization experiment but their relevance to real-life samples is questionable. With this in mind we investigated what would happen if the concentration of a 1-SNP mismatch target was higher than that of the matched target. Hybridization curves are shown in Fig. 8 for a 1:1, 2:1, 5:1, and 10:1 mismatch/match ratio. All of the simulations were done at a temperature of 330 K, the match concentration was set to 100 pM, and were run to simulate 100 h of binding.

The curves shown in Fig. 8 highlight the fact that within 72 h the hybridization experiments have not reached equilibrium, but more interesting is the dynamics of the binding. The 10:1 ratio composite curve growth slows down over short times after the initial jump, but over long hybridization times is actually growing, and in fact the curve is mostly composed of the bound mismatch until ≈30 h have elapsed.

Multiple basepair mismatch

To this point we have only considered the extreme case in which the concentration of a SNP is comparable or higher than the perfect match to be evaluated. However, relevant to the discussion, the situation is less probable than a two- or three-basepair mutation present at concentrations comparable to that of the matched target. The addition of multiple point mutations should change the association rate constant;
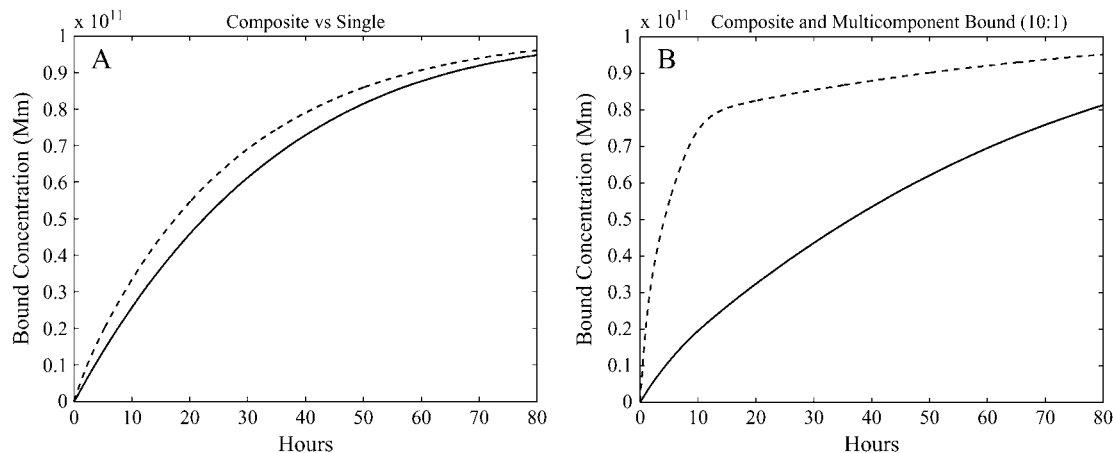

FIGURE 6 Hybridization curves representing the composite curve (*dashed line*) and the actual match target curve for a single-component system (*solid line*) at a temperature of 330 K. (*A*) For a setup with equal 100 pM concentration of match and mismatch. (*B*) For a setup where the match concentration is 100 pM and mismatch concentration is 1 nm.
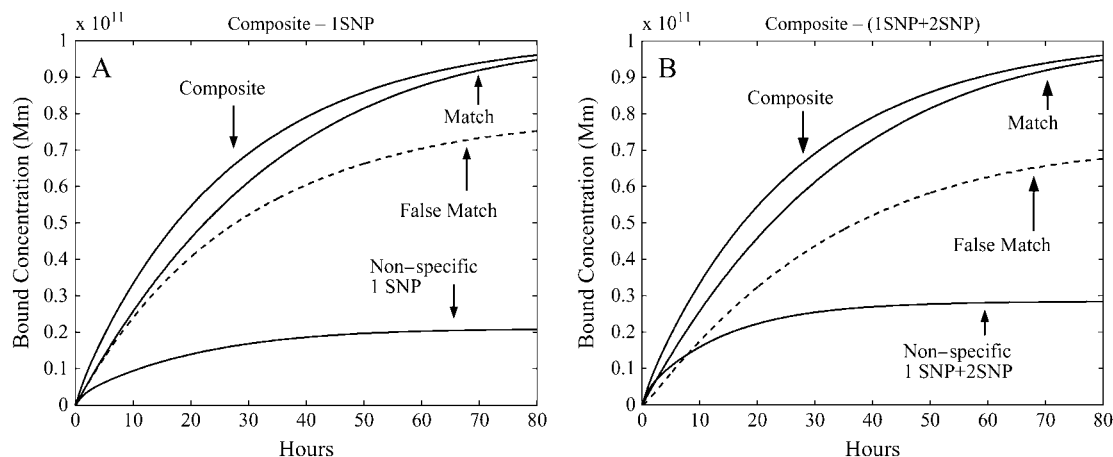
FIGURE 7 Hybridization curves representing the composite curve, actual match target curve, a nonspecific curve, and a false-match curve for simulations performed at equal concentration of 100 pM at a temperature of 330 K. (*A*) Nonspecific, 1 SNP, simulated as a single component. (*B*) Nonspecific, simulated as a two-component solution of 1 SNP and 2 SNP.

however, the magnitude of the change has been suggested to be within one order of magnitude for up to a five-basepair mismatch (14). Simulations were run for a two-base mismatch using equal concentration, 100 pM, of match and mismatch target and association rate constants of 10^6, 5×10^5, and 10^5 M^{-1} s^{-1}. Table 2 shows the dissociation rate constant at a temperature of 330 K for each situation, the bound concentration of match target, bound concentration of mismatch target, and the ratio of bound match/mismatch concentrations. The effects seen from changing the association rate constant on the mismatch-bound concentration are small, and the differences in the calculated dissociation constants vary by less than half an order of magnitude.

Our earlier results in Table 1 show that, to reach thermodynamic equilibrium using picomolar concentrations, experiments would have to run for over 60 h. This time frame is practically unreasonable. We have run simulations to find the point at which the match target is accountable for 90% and 95% of the observed signal. The concentrations of the match and mismatch were fixed at 100 pM while using different

numbers of point mutations and using an association constant of 10^6. Fig. 9 shows that as the number of point mutations grows, the time needed for the match to reach 90% and 95% of the combined signal decreases. This is attributed to the elevated values of dissociation rate constants that accompany the increased number of point mutations, 2 SNP $k_d^{mis} = 7.61 \times 10^{-4}$ s^{-1} and 3 SNP $k_d^{mis} = 1.57 \times 10^{-2}$ s^{-1}—i.e., as the dissociation constant increases, the hybridized pair becomes increasingly unstable. Note that if the concentration of the mismatch is increased, the time to reach the 90% or 95% mark will also increase.

Dynamic range

Determining the dynamic range of sensing on arrays is an issue that has plagued microarray designs. Controlling temperature on the surface of arrays has recently been used as a way to detect sequence mutations by virtue of changing the dissociation rate constants. This mechanism seems to work well as the temperature grows, but the actual dynamic range between the match and mismatch targets decreases. As the temperature is increased, the dissociation constants for match and mismatch increase and converge. Fig. 10 shows the dissociation constants' ratios as a function of temperature. If we assume that the concentrations of the match and mismatch are the same and the association constants are similar, then the ratio of dissociation constants defines the theoretical dynamic range of sensing. The fact is that, at lower temperatures, the dynamic range of match/mismatch discrimination is broader, but the dissociation constants are so small the differences would not be detectable in a realistic time frame.

Using the thermodynamic equilibrium equations for the match target and the corresponding mismatch equation, one can evaluate the theoretical limit of discrimination in

TABLE 1 Time to reach a percentage of thermodynamic equilibrium

Match (pM)/mismatch (pM)	Time 10% (hours)	Time 50% (hours)	Time 90% (hours)
10:0	34.2	NA	NA
10:10	34.4	NA	NA
100:0	3.6	21.3	58
100:100	3.6	22.3	64.1
100:200	3.7	23.7	69.9
100:500	3.9	28.6	83.1
100:1000	4.3	35.7	98
1000:0	0.3	2.0	5.5
1000:1000	1.1	5.5	12.2

Time to reach 10%, 50%, and 90% of thermodynamic equilibrium for different combinations of concentration for the match and mismatch targets.
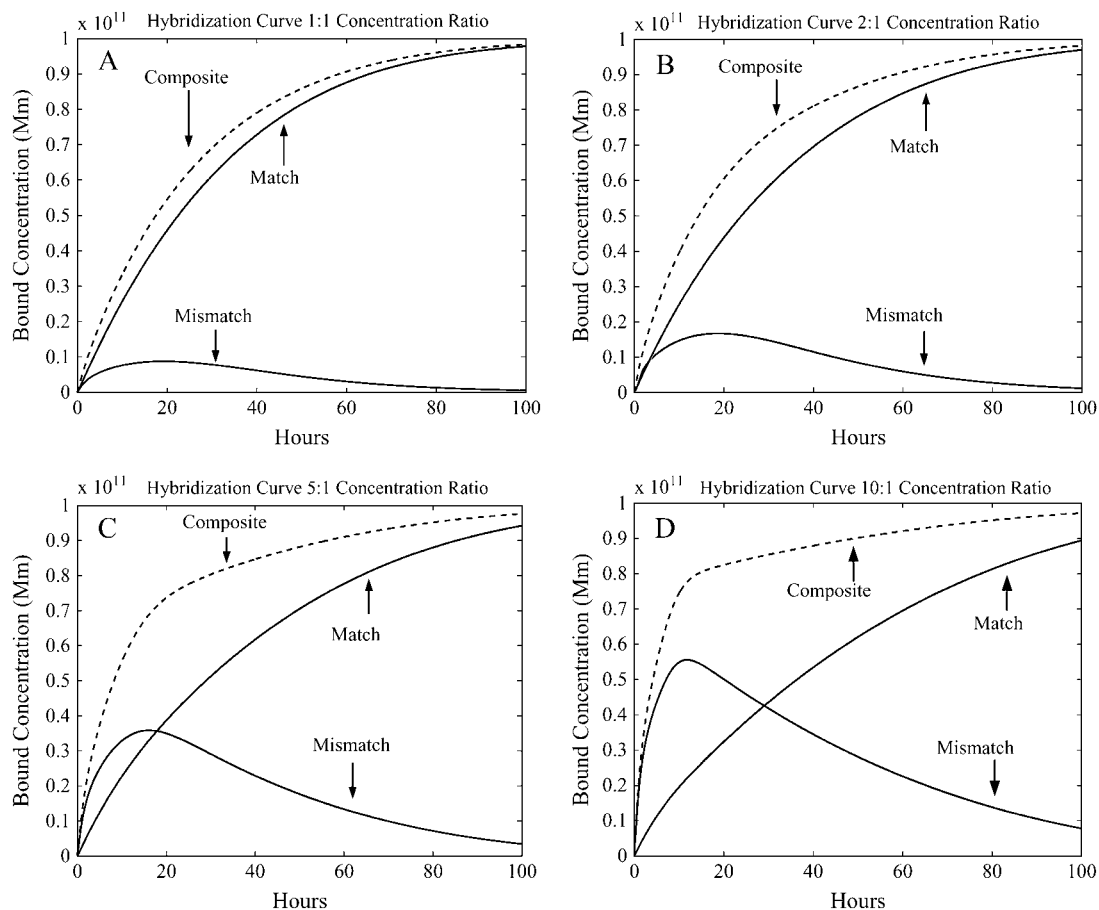
FIGURE 8   Hybridization kinetics representing the match, mismatch, and composite curve. (*A*) Curves with a 1:1 ratio, (*B*) with a 2:1 ratio, (*C*) with a 5:1 ratio, and (*D*) with a 10:1 ratio.

a two-component system. Fig. 11 shows the dynamic range capable on a microarray spot as described by the ratio of bound homoduplex concentration divided by heteroduplex bound concentration at thermodynamic equilibrium,

$$\frac{B^{\mathrm{m}}}{B^{\mathrm{mis}}} = \frac{k_{\mathrm{a}}^{\mathrm{m}} C^{\mathrm{m}} k_{\mathrm{d}}^{\mathrm{mis}}}{k_{\mathrm{a}}^{\mathrm{mis}} C^{\mathrm{mis}} k_{\mathrm{d}}^{\mathrm{m}}}. \tag{12}$$

As the ratio of dissociation rate constants becomes large, simulating an increase in mutations or decrease in temperature, the dynamic range of sensing increases. However, if the concentration of the mismatch is larger than the matched target concentration, the dynamic range decreases. These data demonstrate that there is a point at which the concentration of mismatch can be high enough that discrimination is

no longer plausible. Such a scenario could be created if the combined nonspecifics in a solution had a much higher concentration or an apparent dissociation constant comparable to the match target.

DISCUSSION

When the stationary no-flow technique is used on microarrays, the delivery of target to the sensing surface is accomplished through diffusion. If the affinity reaction on the surface of the array is faster than diffusion, diffusion will control the speed of the surface reaction at the longer times needed to reach the thermodynamic equilibrium of the reaction. This effect is more pronounced when low target concentrations

TABLE 2   Effects of varying association rate constants

Assoc. (M^{-1} s^{-1})	Dissoc. (s^{-1})	Match (Mm)	Mismatch (Mm)	Match/mismatch
1×10^6	7.41×10^{-4}	2.70×10^{-13}	1.61×10^{-13}	1.67
5×10^5	4.05×10^{-4}	2.71×10^{-13}	1.43×10^{-13}	1.89
1×10^5	9.39×10^{-5}	2.71×10^{-13}	9.53×10^{-14}	2.84

Simulation results using different association rate constants for a two-basepair mismatch after simulation of hybridization for 60 min with initial target concentrations of 100 pM.
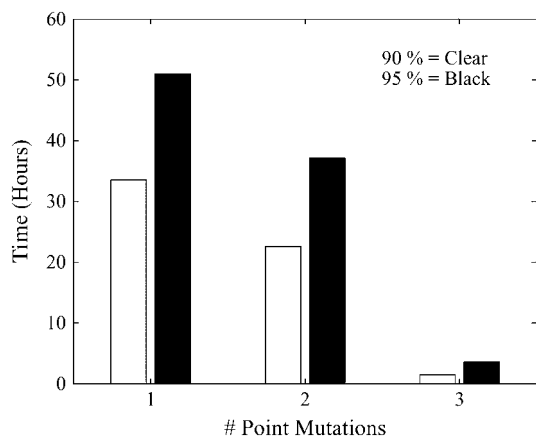
FIGURE 9 Time needed for the match target to reach 90% and 95% of the composite hybridization curve while in a two-component solution of 1-, 2-, or 3-SNP mismatch. Concentrations were equal at 100 pM and dissociation constant calculated at 330 K.

FIGURE 11 Dynamic range achievable at thermodynamic equilibrium using different values of dissociation constant ratios and association constant concentration ratios.

are interrogated. Several models have been created to probe the characteristics of surface binding of DNA. However, the models do not represent the array environment as a multi-component solution. Instead, each target is allowed to enter the system one at a time and targets are not allowed to mix. A similar kinetic model has been suggested for multicomponent systems assuming short time to equilibrium for mismatches compared to matches (27). The model assumes that the nonspecific component reaches a steady-state level which does not change over long hybridization times. Although these assumptions are correct for single-component systems, we show that they may not be true for multicomponent systems, due to competitive binding. Simulations of binding in a two-component system where the concentration of the match and mismatched target are approximately equal have produced hybridization curves indicative of a competitive mechanism of binding.
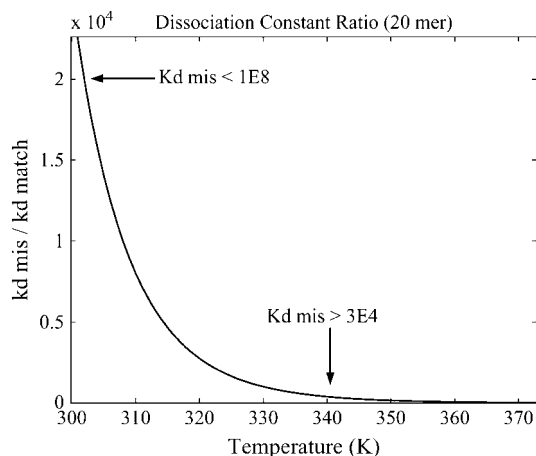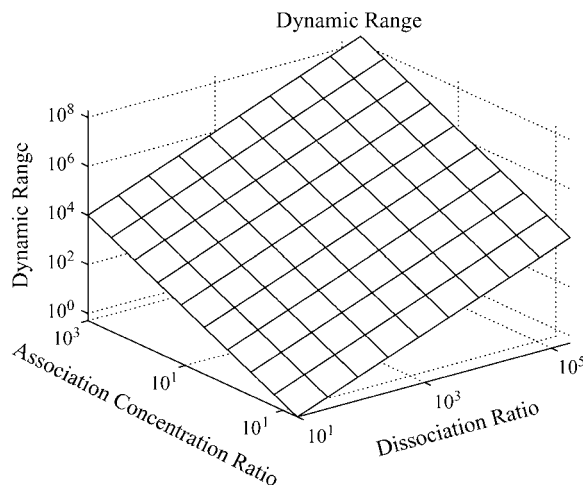

FIGURE 10 Dynamic range achievable at thermodynamic equilibrium using different values of the dissociation constant ratios for a perfectly matched target and a 1-SNP mismatch.

Under the assumptions of the competitive model, surface reactions proceed in two phases. In the early phase, where the amount of bound targets is much lower than the amount of probes available, both matched and mismatched species bind to the sensing surface independently. In the second phase, when the amount of the bound hybrids is comparable to the amount of free probes, the matched species gradually displaces mismatched species from the surface due to higher stability of the homoduplex. This higher stability (or higher affinity) of the matched target is expressed as a significantly lower value of dissociation rate constant compared to the dissociation rate of mismatched species. This was proven by modeling the simultaneous hybridization of both the matched and mismatched targets. Additionally, results presented suggest that it may be more appropriate to consider how groups of targets in a multicomponent solution interact with possible binding sites and not as individual targets.

A recent publication from W. Knoll's group dealt with mass sensing in a two-component system containing wild-type and mutant (truncated) targets in which they considered the way all targets interact with available binding sites (28). Using a similar theoretical model they were able to reconstitute a composite mass sensor signal generated by competitive capture of both targets. However, they did not analyze surface kinetics for each target individually.

One of the important questions raised in this work is: What parameters control time-to-equilibrium during surface hybridization for multicomponent systems? In the case of a single-component system, time-to-equilibrium is defined by the concentration of the target and association and dissociation rate constants: the higher the values of these parameters, the shorter is the time to equilibrium. In the case of a two-component system with competition, the dissociation rate constant of the mismatch emerges as the dominant parameter. Relative concentrations of the species in solution also

affect the time to equilibrium: the higher the relative concentration of the mismatch, the longer is the time to equilibrium. We interpret this result using the competition model: in the early times, mismatch is a dominant bound species because it has a higher concentration; in the later stages of reaction, the rate of mismatch displacement by the match is dominated by the rate of mismatch dissociation.

Microarray analysis has become increasingly complex due to the growing size of arrays and the inherent cross-binding of targets. Several researchers have suggested that cross-binding can be accounted for analytically, using probe sites specifically designed to capture nonspecific targets (29–31). This is done by subtracting the nonspecific signal from the signal produced by the perfectly matched target. The non-specific spot arrangement has been tested experimentally and has frequently produced erratic results (19,26,29). One common feature, which allows us to explain the origins of these discrepancies, is rooted in the equilibrium approximation, where surface concentrations of targets follow Langmuir or modified Langmuir isotherm (24,32,33). Researchers generally allow a microarray experiment to proceed for between 16 and 48 h at a time and at that point assume that the surface reaction is complete. Our results suggest that at low concentrations, which were used for equilibrium analysis based on the Affymetrix database, time-to-equilibrium may be on the order of hundreds of hours, so an equilibrium approach to analysis of microarray data should be used with caution. Experimental study of hybridization kinetics in multicomponent systems also indicates continuing growth of specific target surface concentration after 72 h of hybridization, in agreement with our theoretical predictions (27). Wu et al. (32) have performed analysis of experimental results that assumes negligible contribution of SNPs to cross-hybridization. However, kinetic studies performed by Erickson et al. (12) clearly indicate significant contribution of SNPs to the target signal in the kinetic regime. The example of SNP, analyzed in this study, represents a centrally positioned mismatch. As was previously shown, surface-bound oligonucleotides exhibit stronger dependence on the mismatch position than during solution hybridization (34). With less destabilizing mismatches, resulting in higher affinities of mismatched species, competitive effects will be even more prominent. Our competitive model, corroborating kinetic experimental results, allows us to further understand why erratic results have been produced by looking at kinetic curves during hybridization.

CONCLUSION

Using a two-component model we have presented results describing kinetic behaviors of matched and mismatched targets at the sensing zone. Even though the model does not simulate a complete array, the effects of competitive binding would increase as the simulated size of the array increases. Under common conditions of a microarray experiment we have shown that low initial target concentrations require longer times to reach thermodynamic equilibrium than are usually allowed and therefore contribution of mismatched targets to the observed signal may be significant. Moreover, even minor variations in hybridization times may cause significant shifts in match/mismatch ratio. We have presented some mechanisms that could explain the inconclusive published data concerning the use of mismatched sensing spots to quantify the amount of nonspecific binding on the array. Based on our virtual experiments it is plausible to suggest that not only single nucleotide mismatches but multiple point mutations may have significant affinity to the sensing zones, thus altering quantitative assessments. Results shown here indicate that if the mismatches in solution are at equal or higher effective concentrations than the matched species, then the use of nonspecific spots will produce errors. The error produced will be directly dependent on the temperature at which the experiment is done, the sequence to be investigated, and the design of the nonspecific spot. Further simulations and experiments are needed to expand the competitive model to real-size DNA arrays. However, even the simple case presented here demonstrates capabilities of the competitive model to explain complex dynamics of the target capture and identify critical parameters of microarray experiments.

Note added in proof: Another recent study (35) has also presented a competitive model of DNA hybridization.

REFERENCES

1. Maron, B. J., J. H. Moller, C. E. Seidman, G. M. Vincent, H. C. Dietz, A. J. Moss, H. M. Sondheimer, R. E. Pyeritz, G. McGee, and A. E. Epstein. 1998. Impact of laboratory molecular diagnosis on contemporary diagnostic criteria for genetically transmitted cardiovascular diseases: hypertrophic cardiomyopathy, long-QT syndrome, and Marfan syndrome. *Circulation*. 98:1460–1471.

2. Hacia, J. G. 1999. Resequencing and mutational analysis using oligonucleotide microarrays. *Nat. Genet.* 21:42–47.

3. Raychaudhuri, S., P. D. Sutphin, J. T. Chang, and R. B. Altman. 2001. Basic microarray analysis: grouping and feature reduction. *Trends Biotechnol.* 19:189–193.

4. Kumar, A., G. Goel, E. Fehrenbach, A. K. Puniya, and K. Singh. 2005. Microarrays: the technology, analysis and application. *Eng. Life Sci.* 5:215–222.

5. Edwards, D. A. 2000. Biochemical reactions on helical structures. *SIAM J. Appl. Math.* 60:1425–1446.

6. Mason, T., A. R. Pineda, C. Wofsy, and B. Goldstein. 1999. Effective rate models for the analysis of transport-dependent biosensor data. *Math. Biosci.* 159:123–144.

7. Wang, J., and K. Drlica. 2003. Modeling hybridization kinetics. *Math. Biosci.* 183:37–47.

8. Vijayendran, R. A., F. S. Ligler, and D. E. Leckband. 1999. A computational reaction-diffusion model for the analysis of transport limited kinetics. *Anal. Chem.* 71:5405–5412.

9. Zimmermann, M., E. Delamarche, M. Wolf, and P. Hunziker. 2005. Modeling and optimization of high-sensitivity, low-volume microfluidic-based surface immunoassays. *Biomed. Microdev.* 7:99–110.

10. Sorokin, N. V., V. R. Chechetkin, M. A. Livshits, V. A. Vasiliskov, A. Y. Turygin, and A. D. Mirzabekov. 2003. Kinetics of hybridization on the oligonucleotide microchips with gel pads. *J. Biomol. Struct. Dyn.* 21:279–288.

11. Chan, V., D. J. Graves, P. Fortina, and S. E. McKenzie. 1997. Absorption and surface diffusion of DNA oligonucleotides at liquid/solid interfaces. *Langmuir.* 13:320–329.

12. Erickson, D., D. Li, and U. Krull. 2003. Modeling of DNA hybridization kinetics for spatially resolved biochips. *Anal. Biochem.* 317:186–200.

13. Hagan, M. F., and A. K. Chakraborty. 2004. Hybridization dynamics of surface immobilized DNA. *J. Chem. Phys.* 120:4958–4968.

14. Heule, M., and A. Manz. 2004. Sequential DNA hybridisation assays by fast micromixing. *Lab Chip.* 4:506–511.

15. Myszka, D. G., X. He, M. Dembo, T. A. Morton, and B. Goldstein. 1998. Extending the range of rate constants available from biacore: interpreting mass transport-influenced binding data. *Biophys. J.* 75:583–594.

16. Okahata, Y., M. Kawase, K. Niikura, F. Ohtake, H. Furusawa, and Y. Ebara. 1998. Kinetic measurements of DNA hybridization on an oligonucleotide-immobilized 27-mHz quartz crystal microbalance. *Anal. Chem.* 70:1288–1296.

17. Henry, M. R., P. W. Stevens, J. Sun, and D. M. Kelso. 1999. Real-time measurements of DNA hybridization on microparticles with fluorescence resonance energy transfer. *Anal. Biochem.* 276:204–214.

18. Sekar, M. M. A., W. Bloch, and P. M. S. John. 2005. Comparative study of sequence-dependent hybridization kinetics in solution and on microspheres. *Nucleic Acids Res.* 33:366–375.

19. Levicky, R., and A. Horgan. 2005. Physicochemical perspectives on DNA microarray and biosensor technologies. *Trends Biotechnol.* 23:143–149.

20. SantaLucia, J. 1998. A unified view of polymer, dumbbell, and oligonucleotide DNA nearest-neighbor thermodynamics. *Biochemistry.* 95:1460–1465.

21. Ikuta, S., K. Takagi, R. B. Wallace, and K. Itakura. 1987. Dissociation kinetics of 19 basepaired oligonucleotide-DNA duplexes containing different single mismatched basepairs. *Nucleic Acids Res.* 15:797–811.

22. Dimitrov, R. A., and M. Zuker. 2004. Prediction of hybridization and melting for double-stranded nucleic acids. *Biophys. J.* 87:215–226.

23. Markham, N. R., and M. Zuker. 2005. DINAMelt web server for nucleic acid melting prediction. *Nucleic Acids Res.* 33:W577–W581.

24. Halperin, A., A. Buhot, and E. B. Zhulina. 2004. Sensitivity, specificity, and the hybridization isotherms of DNA chips. *Biophys. J.* 86:718–730.

25. Peterson, A. W., R. J. Heaton, and R. M. Georgiadis. 2001. The effects of surface probe density on DNA hybridization. *Nucleic Acids Res.* 29:5163–5168.

26. Peterson, A. W., L. K. Wolf, and R. M. Georgiadis. 2002. Hybridization of mismatched or partially matched DNA at surfaces. *J. Am. Chem. Soc.* 124:14601–14607.

27. Dai, H., M. Meyer, S. Stepaniants, M. Ziman, and R. Stoughton. 2002. Use of hybridization kinetics for differentiating specific from nonspecific binding to oligonucleotide microarrays. *Nucleic Acids Res.* 30:E86.

28. Tawa, K., D. Yao, and W. Knoll. 2005. Matching basepair number dependence of the kinetics of DNA-DNA hybridization studied by surface plasmon fluorescence spectroscopy. *Biosens. Bioelectron.* 21:322–329.

29. Naef, F., D. A. Lim, N. Patil, and N. Magnasco. 2002. DNA hybridization to mismatched templates: a chip study. *Phys. Rev. E.* 65:040902–1–040902–4.

30. Lockhart, D. J., and E. A. Winzeler. 2000. Genomics, gene expression and DNA arrays. *Nature.* 405:827–836.

31. Lipshutz, R. J., S. P. A. Fodor, T. R. Gingeras, and D. J. Lockhart. 1999. High density synthetic oligonucleotide arrays. *Nat. Genet.* 21:20–24.

32. Wu, C., R. Carta, and L. Zhang. 2005. Sequence dependence of crosshybridization on short oligo microarrays. *Nucleic Acids Res.* 33:e84. Published online 2005 May 24. DOI: 10.1093/nar/gni082.

33. Mei, R., E. Hubbell, S. Bekiranov, M. Mittmann, R. C. Christians, M. Shen, G. Lu, J. Fang, W. Liu, T. Ryder, P. Kaplan, D. Kulp, and T. A. Webster. 2003. Probe selection for high-density oligonucleotide arrays. *Proc. Natl. Acad. Sci. USA.* 100:11237–11242.

34. Zhang, L., M. F. Miles, and K. D. Aldape. 2003. A model of molecular interactions on short oligonucleotide microarrays. *Nat. Biotechnol.* 21:818–821.

35. Zhang, Y., D. A. Hammer, and D. J. Graves. 2005. Competitive hybridization kinetics reveals unexpected behavior patterns. *Biophys. J.* 89:2950–2959.